J.P

# Cosmic ray plasma of leptons, protons and $^4$He

LBNL 52116

T. F. Hoang

*Lawrence Berkeley National Laboratory, Berkeley, Ca 94720*

*University of California, Space Science Laboratory, Berkeley, Ca 94720*

**Abstract**

The momentum distributions of high altitude cosmic ray particles from the AMS, the CAPRICE and the MASS Collaboration are analyzed using the lognormal distribution. The average momentum is found to be the same, $P_0 = 2.225 \pm 0.072$ GeV/c, for $e^{\pm}$, $\mu^-$, p and $^4$He/ nucleon. This property implies that the particles are accelerated through equipartition of momentum once trapped by the geomagnetic fields in the interstellar space to form cosmic plasmas. The plasma temperature estimated from $P_0$ is $218 \pm 18$ MeV. Its distance to the experimental setup is $\sim 14$ km according to the muon lifetime, so that these particles originate at the top of the atmosphere near the detectors.

# 1 Introduction

The characteristic feature of the energy spectrum of cosmic ray particles is the knee, i.e. break of the power law $E^{-\gamma}$ predicted by the Fermi mechanism for cosmic ray particle production [1,2]. In a recent satellite experiment of high statistics, the AMS Collaboration reported the spectral index $\gamma_p = 2.78 \pm 0.02$ for protons of momentum in a range from 10 to 200 GeV/c [3] and about the same for $^4$He [4]. Indeed, we shall see that the shape of these two distributions is actually very similar. Whereas for electrons and positrons [5] the shape of the spectrum is quite different, the maximum being much more pronounced and the width much narrower [6]. The existence of a maximum in the energy spectrum rules out the power law behavior in the lower energy region. It is a challenge to interpret the spectrum of these cosmic ray particles in the entire energy range, including the region of the maximum of distribution. As the log plots are similar to parabolas, therefore it is appropriate to describe the spectra with lognormal distributions.

As the production mechanism of electrons and positrons is quite different from that of protons, the determination of their origin requires a knowledge of dynamical properties of their production. An attempt is therefore made to investigate the production of cosmic ray particles by analyzing their momentum distributions with a lognormal distribution (Sect. 2), i.e. a Gaussian distribution in terms of the random kinematic variable Log P, which represents the invariant phase-space of the particle under consideration. This amounts to assume that the production process is stochastic, just like the partition temperature model of Chou, Yang and Yen [7], in view of the complexity of the acceleration of cosmic ray particles, which may take place in various ways, besides the Fermi mechanism. We then estimate the average momentum of the spectrum to investigate the production property. The properties of the lognormal distribution applied to the particle production will be discussed in the Appendix.

The average momentum $< P >$ thus estimated will be tested by a method based on the dependence of $< P >$ on the cut-offs on the momentum range of measurement. The behavior of $< P >_{cut}$ thus estimated is found to follow an exponential law of probability. In this way, we find about the same $< P >$ for protons and $^4$He/nucleon (Sect. 3), as well as for electrons and positrons (Sect. 4). This property holds also for muons and electrons of high altitude balloon experiments at different time and different location of the CAPRICE Collaboration [8] (Sect. 5). Furthermore, the muons from different altitudes are found to have also about the same average momentum Sect. 6).

Therefore the equipartition of momentum holds for the production these cosmic ray particles measured of the AMS Collaboration [1-3] and the CAPRICE Collaboration [8], the mean value being $P_0 = 2.232 \pm 0.098$ GeV/c. The acceleration process takes place when the charged particles are trapped inside a plasma formed by the electromagnetic fields in the interstellar space through equipartition of momentum for the trapped particles (Sect. 6).

Remarks will be made on the universality of the average momentum of particles from cosmic ray plasmas. It allows to determine the characteristics of the plasma: the temperature $\sim$ 217 Mev comparable to the critical temperature of quark-gluon plasma. It is a very hot plasma, like a heat sink to establish momentum equipartition of particles enclosed inside the plasma. The plasma is $\sim$ 14 km above the setups of the AMS and CAPRICE experiments according to the lifetime of the observed muons(Sect. 6), indicating that the muons, therefore the pions, originate at the top of the atmosphere.

## 2 Protons

Consider first the protons as measured by the AMS Collaboration [3] at an altitude of 350 to 390 km, corresponding to 3.5 g/cm$^2$ residual atmosphere, with $\sim 10^7$ events covering a wide range of kinetic energy from 0.1 to 200 GeV. The momentum distribution according to their data is shown in Fig. 1. The curve represents a least-squares fit with a lognormal distribution in terms of the invariant phase space of the particle denoted by

$$\zeta = \text{Log P (GeV/c)}, \tag{1}$$

so that

$$\frac{dn}{dP} = \text{N}e^{-(\zeta+\zeta^*)^2/2L}. \tag{2}$$

The parameters are $\zeta^*$, the shift of the maximum and L, the width of the distribution, N being the normalization. The properties of this distribution will be discussed in the Appendix. We use common logarithms for the fit and find, N in units of $(m^2 sec\ sr\ MeV)^{-1}$,

$$\zeta^*_p = 1.046 \pm 0.056,\ \text{L}_p = 0.379 \pm 0.010,\ \text{N}_p = 7.11 \pm 1.11.$$

The average momentum computed according to the fit yields

$$< \text{P} >_p = 2.316 \pm 0.022\ \text{GeV/c}. \tag{3}$$

and the standard deviation

$$\sigma_p = 4.980\ \text{GeV/c}.$$

A comparison with the data indicates that, in general, the fit is rather good up to P $< 50.4\ GeV/c$, far away from the average $<$ P $>$, including $\sim$ 99.85 percent of the data.

As the tail of the lognormal distribution is higher than in the case of Gaussian distribution, we have to investigate its effect on the estimation of $<$ P $>$ by cutting off successively the momentum range. The values of $<$ P $>_{cut}$ thus obtained for P $<$ P$_{cut}$ are shown by triangles in Fig. 2. We see a drastic drop (filled triangles) to a minimum around P$_{cut} \sim$ 4.89GeV/c, then a gradual rise (open triangles) to reach a

plateau. Leaving aside the falling part of points and limiting ourselves to the rising part of data with $P_{cut} > 5$ GeV/c, we find its behavior following an exponential law of Poisson, namely

$$< P >_{cut} = C(1 - e^{-cP_{cut}}). \quad (4)$$

as shown by the curve with

$$c_p = 0.243 \pm 0.013 \ (GeV/c)^{-1}, \ C_p = 2.113 \pm 0.021 \ GeV/c.$$

We see that $< P >_{cut} = 0$ for $P_{cut} = 0$ as should be and that its rise at a rate $\Delta < P >_{cut} / \Delta P_{cut} \simeq 8.5$ to approach asymptotically a plateau at the ordinate given by $C_p$ corresponding to the exact value for the average of momentum in agreement with the estimate (3) without cuts.

We note in passing that this method of cutoff will be useful for a reliable estimation of the average momentum, when the measurements cover only a limited range of momentum as in the case of positrons to be discussed later in Sect. 4.

# 3 Helium

Next, let us turn to the primary $^4$He of the AMS experiment [4]. We reproduce in Fig. 3 their distribution as a function of the momentum measured by the rigidity (in GV) as reported in [4]. A least-squares fit according to the lognormal distribution (2) is shown by the solid curve in the figure with

$$\zeta^*_{He} = 0.460 \pm 0.026, \ L_{He} = 0.315 \pm 0.016, \ N_{He} = 106.88 \pm 5.80.$$

N being in units of $(m^2 \, sec \, sr \, GeV/c)^{-1}$. This fit is comparable to the proton case as presented in the previous section.

From the momentum of $^4$He measured by the AMS magnetic spectrometer, we find its average per nucleon

$$< P >_{He} = \frac{2}{4}(4.558 \pm 0.021) = 2.279 \pm 0.010 \ \text{(GeV/c)/nucleon}, \quad (5)$$

just like the protons (3) within fitting errors and the standard deviation per nucleon, so is the standard deviation

$$\sigma_{He} = 2.248 \ GeV/c.$$

The effect of cutoffs on the momentum range is shown by circles in Fig. 2. The plot resembles that for protons (in triangles) in the same figure, namely an abrupt drop (in filled circles) to a minimum, then a rise (open circles) as is described by an exponential law (4) with

$$c_{He} = 0.196 \pm 0.0103 \, (GeV/c)^{-1}, \ C_{He} = 4.473 \pm 0.008 \, GeV/c. \quad (6)$$

Note the ratio of coefficients C for protons and helium

$$\frac{C_{He}}{C_p} = 2.117 \pm 0.017,$$

is in agreement with that of the nuclear charge Z to the atomic number A for He and p. This indicates that the average momentum of He per nucleon is the same as that of proton. As for the flux ratio, we find it by integrating the distribution (2) to get

$$\frac{^4\mathrm{He}}{\mathrm{p}} = \frac{258.0 \pm 8.9}{4645 \pm 423} = 0.056 \pm 0.006, \tag{7}$$

about 6 per cent.

# 4 Electrons and positrons

The dynamical properties of electrons and positrons present special interest, as far as their origin is concerned. Unlike the protons, they are not from the primary production. They are rather related to other particles, namely $\pi^0 \to \gamma + \gamma$ with $\gamma \to e^+ + e^-$, so that $< \mathrm{P} >_e = \frac{1}{4} < \mathrm{P} >_\pi$ with $< \mathrm{P} >_\pi \simeq \frac{2}{3} < \mathrm{P} >_p$ ( cf. Appendix).

On the other hand, electrons, positrons and protons may be accelerated by geomagnetic field in the interstellar space. Furthermore, as charged particles, they may interact among themselves by Coulomb force to reach an equilibrium characterized by the same $< \mathrm{P} >$, as is required by the equipartition of momentum.

The electrons and the positrons measured by the AMS Collaboration [5] at an altitude 320 to 390 km in the range P = 0.2 to 40 GeV/c for electrons (in circles) and 0.3 to 3 GeV/c for positrons (in nablas) are reproduced in Fig. 4. The curves are fits according to the lognormal distribution (2).

Consider first the electrons, the parameters (N in $(m^2\, sec\, sr\, MeV/c)^{-1}$)

$$\zeta^*_{e^-} = 0.124 \pm 0.025,\ \mathrm{L}_{e^-} = 0.135 \pm 0.010,\ \mathrm{N}_{e^-} = 0.0217 \pm 0.018.$$

We find for the average momentum

$$< \mathrm{P} >_{e^-} = 2.153 \pm 0.118,\ GeV/c, \tag{8}$$

and the standard deviation

$$\sigma_e = 2.251\ GeV/c,$$

both comparable to the case of protons (3), despite the striking difference in the shape of their spectrum, as indicated by the difference of their width parameter: $\mathrm{L}_{e^-}/\mathrm{L}_p = 2.81 \pm 0.10$.

The averages $< \mathrm{P} >_{cut}$ with cutoffs on P are shown by circles in Fig. 5. The fit is shown by the dashed line in the figure with

$$\mathrm{c}_{e^-} = 1.113 \pm 0.026\,(GeV/c)^{-1},\ \mathrm{C}_{e^-} = 1.861 \pm 0.082\,GeV/c.$$

Note that the asymptotic value $C_{e^-}$ is close to the average momentum (8).

Next, let us turn to the positrons as shown by the triangles in Fig. 4. Here, the data cover only a limited range from P = 0.2 to 3 GeV/c. The curve shows the fit with

$$\zeta^*_{e^+} = 0.413 \pm 0.154,\ L_{e^+} = 0.233 \pm 0.108,\ N_{e^+} \sim 0.041,$$

the estimate of the normalization coefficient N is uncertain as the error is very large.

None-the-less, we may estimate a lower limit of the average momentum and get:

$$< P >_{e^+} \succ 1.313 \pm 0.078\ GeV/c. \tag{9}$$

The values of $< P >_{cut}$ for cutoffs on P are shown by the triangles in Fig. 5. The solid curve represents the exponential rise according to (5), with

$$c_{e^+} = 0.673 \pm 0.0152\,(GeV/c)^{-1},\ C_{e^+} = 1.787 \pm 0.242\,GeV/c.$$

It is interesting to note that $C_{e^+} \simeq C_{e^-}$, whereas $c_{e^+} \ll c_{e^-}$, because of annihilations with electrons and different cuts by the magnetic field of the earth, and that the flux of $e^-$ in the same range P = 0.2 to 3 GeV/c is found to be about one order of magnitude larger than that of $e^+$ as is shown in Fig. (4). Now, if we refit the $e^-$ data in the same range as $e^+$, i.e. filled circles in the figure, we then get

$$c'_{e^-} = 2.011 \pm 0.207\,(GeV/c)^{-1},\ C'_{e^-} = 1.781 \pm 0.014\ GeV/c.$$

We find the same value C for both $e^+$ and $e^-$, namely $C_{e^+} = C'_{e^-}$. This gives strong indication that the average momentum of positrons is essentially the same as those of electrons, protons and $^4$He per nucleon , if there were no loss by annihilations, no cuts by the magnetic field of the earth.

# 5 Muons

We now turn to the muons and the electrons of cosmic rays at high altitude corresponding to 3.8 g/cm$^2$ of the balloon-flight experiments by the CAPRICE Collaboration [8] as shown in Fig. 6. As the muons arise mainly from the $\beta$-decays of $\pi^\pm \rightarrow \mu^\pm + \nu$, their spectrum is similar to that of $\gamma's$ from the decays of $\pi^0 \rightarrow \gamma + \gamma$. Whereas the electrons are from $\gamma \rightarrow e^+ + e^-$. Therefore, there is a correlation of 2 to 1 ratio between the widths of the muon and the electron spectrum as is known in the case of particle production by $e^+e^-$ interactions (cf. Appendix).

The momentum spectrum of $\mu^-$ (in circles) and $e^-$ (in triangles) are shown in Fig. 6. The curves represent the least-squares fits with the lognormal distributions Eq. (2). The parameters for $\mu^-$ are (N in $(m^2\ \text{sec sr}\ GeV/c)^{-1}$)

$$\zeta^*_{\mu} = 1.133 \pm 0.116,\ L_{\mu} = 0.330 \pm 0.028,\ N_{\mu} = (3.085 \pm 0.691)/10^3,$$

leading to

$$< \mathrm{P} >_{\mu} = 2.163 \pm 0.205\, GeV/c, \tag{10}$$

and

$$\sigma_{\mu} = 3.881\ GeV/c.$$

Whereas for the electrons

$$\zeta^*_e = 0.162 \pm 0.028,\ \mathrm{L}_e = 0.140 \pm 0.007,\ \mathrm{N}_e = 14.81 \pm 0.73$$

and

$$< \mathrm{P} >_{e} = 2.307 \pm 0.004\, GeV/c. \tag{11}$$

with

$$\sigma_e = 2.038\ GeV/c.$$

The shapes of these two distributions are quite different. However, we find

$$\frac{\mathrm{L}_{\mu}}{\mathrm{L}_e} = 2.359 \pm 0.232,$$

consistent with 2 within about one and a half standard deviations as expected from the property of the width parameter as mentioned above. On the other hand, we find

$$< \mathrm{P} >_{\mu} \simeq < \mathrm{P} >_{e}\ . \tag{12}$$

within $\sim 1/2$ standard deviation, in contradistinction with $< \mathrm{P} >_{\mu} = 2 < \mathrm{P} >_{e}$ as expected from $\pi$ production by high energy interactions, see Appendix. In this case the ratio of numbers of electrons and muons from $\pi^0$ and $\pi^-$ decays should be $n_e/n_{\mu} = 2/1$.

However, here, we find by integrating the distributions in Fig. 6

$$\frac{n_e}{n_{\mu}} = 3.961 \pm 0.321, \tag{13}$$

significantly larger by a factor of $\sim 2$.

Indeed, the excess of electrons observed in this experiment may arise from the decays of $\mu^- \rightarrow e^- + \nu + \bar{\nu}$ during the lapse of time between the production of $\pi$'s and the trapping by the plasma of the decay electrons of $\mu$'s from $\pi \rightarrow \mu + \nu$ decays. Let $f$ denote the fraction of these $\mu$ decays into electrons, then $n_e/n_{\mu} = (2+f)/(1-f)$ leading to

$$f = 0.395 \pm 0.321.$$

As muons are short lived particles, their distance to the experimental setup should be within their decay mean-free-path, namely $(\gamma c\tau)_{\mu} \simeq 14$ km, $\gamma$ being the Lorentz factor of muons $\gamma_{\mu} = < P >_{\mu} / m_{\mu} = 20.600 \pm 1,952$, so that they are produced at the top of the atmosphere.

It is remarkable that the average momentum of electrons of this experiment (11) is comparable with that of the AMS experiment (8) as discussed in the previous section, despite the year and the location of these two experiments are quite different.

# 6 Momentum equipartition in Cosmic Ray plasma

We have seen in the previous sections that the average momentum of cosmic ray particles at high altitude of 390 km is practically the same for leptons, protons and $^4$He/nucleon. This property is in contrast with that of particle production by high energy interactions as discussed in the Appendix. We have to investigate if there is any altitude effect to cause this difference.

For this purpose, we analyze the negative muons at various altitudes of another balloon-flight experiment in 1991 by the MASS Collaboration [9]. Their data are shown in Fig. 7, the errors bars being imperceptible. The curves represent the lognormal fits with Eq. (2). The parameters are listed in Table I,

Table I- Parameters of lognormal fits to muon spectra

| x(g/cm$^3$) | $\zeta^*$ | L | N | $< P >$(GeV/c) |
|---|---|---|---|---|
| 25 - 47 | 0.674 $\pm$ 0.086 | 0.253 $\pm$ 0.020 | (1.83 $\pm$ 0.07)/$10^4$ | 1.910 $\pm$ 0.012 |
| 48 - 83 | 0.700 $\pm$ 0.156 | 0.252 $\pm$ 0.036 | (1.12 $\pm$ 0.13)/$10^3$ | 1.701 $\pm$ 0.406 |
| 83 - 106 | 0.510 $\pm$ 0.079 | 0.213 $\pm$ 0.018 | (1.12 $\pm$ 0.30)/$10^2$ | 1.931 $\pm$ 0.484 |
| 106 - 164 | 0.560 $\pm$ 0.107 | 0.231 $\pm$ 0.025 | (1.42 $\pm$ 0.13)/$10^2$ | 2.003 $\pm$ 0.493 |
| 164 - 255 | 0.511 $\pm$ 0.062 | 0.265 $\pm$ 0.037 | (1.09 $\pm$ 0.29)$10^2$ | 2.647 $\pm$ 0.265 |

A comparison of the parameters $\zeta^*$ and L indicates that they are all the same within fitting errors, except the normalization coefficients N. These parameters are comparable with those of muons at a much higher altitude, about 3.8 g/cm$^3$, of the CAPRICE experiment analyzed in the previous section. The same property holds for the average momentum in the last column of the Table, indicating no altitude effect on the muon momentum distributions we have analyzed.

However, their intensities vary with the altitude, as is seen from the values of N. As for the flux, we may integrate the momentum distributions according to the fits. The results thus obtained are shown in semi-log plot of Fig. 8. The curve is a linear fit assuming the muon flux to be proportional to the atmosphere above the setup of the experiment

$$n_\mu = \frac{x}{\lambda}. \tag{14}$$

We find for the attenuation mean-free-path

$$\lambda = 7205 \pm 167\,\mathrm{g/cm^3},$$

very large indeed, in contrast with the mean-free-path $\sim 60$ g/cm$^3$ for pion production by high energy nucleon-nucleon collisions. This indicates that the muons, therefore the pions, are produced in the atmosphere.

Finally, a comparison of the values of $< P >$ in the Table indicates that they are practically all the same within fitting errors, the mean value $2.044 \pm 0.332$ being comparable with the average momentum of $e^\pm$, p and $^4$He/nucleon mentioned in the

previous sections.

We therefore find an important dynamical property of equipartition of momentum for the acceleration charged cosmic ray particles of the Fermi model [1], namely the acceleration proceeds via electromagnetic interaction of long range with the wandering geomagnetic field in the interstellar space to form a plasma so that once the particles trapped inside, they may gain energy from that of the geomagnetic field through equipartion of momentum, then escape the plasma and continue their motion along the lines of force of the geomagnetic field in the direction of the propagation of the longitudinal waves of the geomagnetic field towards the earth in the form of cosmic ray jets.

As the transverse momentum of particles in a jet is negligible, their average momentum is actually given by $< P >$, which represents the partition temperature of the Chou, Yang and Yen model [7].

# 7 Conclusions

We have used the lognormal distribution Eq.(2) to analyze the momentum spectrum of high altitude cosmic ray leptons, protons and $^4$He of the satellite experiment by the AMS Collaboration [3-5] as well as electrons and muons of the balloon flight experiment by the CAPRICE Collaboration [8]. The average momentum of $e^{\pm}$ and $\mu^-$ is found to be about the same for p and $^4$He/nucleon, their mean value denoted by subscript zero being

$$\mathrm{P}_0 = 2.225 \pm 0.072 \; GeV/c. \tag{15}$$

Whereas the average momentum of negative muons at various altitudes between 25 and 255 g/cm$^3$ of the MASS Collaboration [9] is found to be consistent with this mean value $\mathrm{P}_0$.

This property is of fundamental importance for the production of high altitude cosmic ray particles. As it is different from that by high energy accelerator. Indeed, in the latter case, the average momentum of electrons, is very different from that of protons, as they arise from decays of $\pi^0 \rightarrow \gamma + \gamma$ followed by $\gamma \rightarrow e^+ + e^-$, as discussed in the Appendix. On the contrary, the dynamical property according to (15) implies equipartition of momentum for all these cosmic ray particles observed in the two different experiments. As they are charged particles, it is through their electromagnetic interaction of long range force with the geomagnetic fields in the interstellar space that they form altogether cosmic ray plasmas to establish momentum equipartition among particles once trapped inside the plasma.

This property (15) is universal. It holds also for antiprotons and protons as well, as has been found in another high altitude balloon flight experiment at different place and different time, the BESS Collaboration [10], namely $< \mathrm{P} >= 2.184 \pm 0.056$ GeV/c for protons and $2.666 \pm 0.218$ GeV/c for antiprotons, as reported elsewhere [11].

We therefore have the strong support that the average momentum $P_0 = 2.225$ GeV/c is characteristic of particle production by cosmic ray plasmas.

As regards the properties of the plasma, we note that its temperature T may be estimated from the energy dependence of the average momentum, just like the average multiplicity, namely $< P > \sim \sqrt{E_{cm}}$ according to the Fermi-Landau law [12,13]. The universality of this remarkable law [14a] allow us to estimate the temperature of the cosmic ray plasma knowing the $< P >_p$ of protons and the equilibrium temperature of $e^+e^- \rightarrow$ hadrons at $E_{cm} = 29$ GeV as reported before [14b] and $< P >_p$ as listed in the Table of the Appendix, . We find by scaling

$$T = (0.196 \pm 0.007)\sqrt{\frac{2.225 \pm 0.072}{1.806 \pm 0.062}} = 0.218 \pm 0.018 \text{ GeV} \tag{16}$$

comparable to the critical temperature $\sim$ 250 MeV of quark-gluon plasma. It is a very hot plasma indeed. It severs as a huge reservoir of great heat capacity for the latent energy from the wandering geomagnetic fields for the acceleration of charged particles once trapped inside the plasma in order to establish equipartition of momentum among the trapped particles.

As the muons are short lived, the time for the equipartition process should be accomplished within the lifetime of muons, namely $(\gamma c\tau)_\mu = 46.51$ $\mu$sec, where the Lorentz factor is given by the reduced momentum of muons: $\gamma_\mu = P_0/m_\mu$. Therefore, in the muon experiment, the distance between the plasma and the experimental setup should not exceed the corresponding decay length, namely about 14 km, in other words, these muons are originated in the atmosphere. Therefore, the pions which decay into muons are created in the vicinity of the detector 'at the top of the atmosphere.

But most of these muons at an altitude $\sim$ 40 kms will not reach sea-level, as they are already absorbed by the atmosphere during their traversal towards the Earth. Because their minimum ionization for the air, about 2.5 GeV, exceeds their energy $2.166 \pm 0.205$ they have gained from the heat sink through equipartition of momentum.

Acknowledgements

The author wishes to thank G. F. Smoot for information on the AMS experiment, G.Gidal, I. Hinchliffe, Lifan Wang and Ph. Price for discussions and comments and A. Trattner for help. Thanks to H.J. Crawford for the kind hospitality at LBNL and the Tsi Jung Memorial Fund for the support The work is done through the U.S. Department of Energy Contract No. FG03-90 ER4057.

# 8 Appendix

We have used the lognormal distribution, Eq. (2), to analyze the momentum distributions of Cosmic Ray particles. We now discuss the properties of the parameters $\zeta^*$ and L, characteristics of the distribution.

For this purpose, we consider particles produced by mass-determined inclusive $e^+e^-$ collisions at $E_{cm}$ = 29 GeV of the TPC Collaboration [15] and the HRS Collaboration [16]. The momentum momentum distributions of their measurements are shown in Fig. 9 and 10. The curves represent the least-squares fits with the lognormal distribution Eq. (2). The parameters $\zeta^*$ and L, together with the estimates of the average momentum $< P >$ (in GeV/c) are listed in the following Table.

Table II- Parameters of lognormal fits

| | $\zeta^*$ | L | N | $< P >$ |
|---|---|---|---|---|
| $\pi^+\pi^-$ | 0.642 ± 0.029 | 0.206 ± 0.009 | 1251 ± 54 | 1.231 ±0.008 |
| $K^+K^-$ | 0.286 ± 0.069 | 0.192 ± 0.031 | 0.79 ± 0.74 | 2.186 ± 0.008 |
| p | 0.406 ± 0.237 | 0.204 ± 0.069 | 0.12 ± 0.01 | 1.806 ± 0.062 |
| $\gamma$ | 0.910 ± 0.072 | 0.218 ± 0.015 | 28.75 ± 4.59 | 0.859 ± 0.035 |
| e | -0.007 ± 0.010 | 0.108 ± 0.004 | 4.82 ± 0.05 | 2.80 ± 0.018 |
| $\rho^0$ | -0.282 ± 0.036 | 0.100 ± 0.012 | 0.328 ± 0.022 | 3.362 ± 0.158 |
| $\eta$ | -0.387 ± 0.126 | 0.051 ± 0.021 | 0.167 ± 0.049 | 3.564 ± 0.414 |
| $K^{+*}K^{-*}$ | -0.232 ± 0.067 | 0.085 ± 0.015 | 0.065 ± 0.008 | 3.117 ± 0.138 |

Consider first the width parameter L for pions, kaons and protons, we find practically the same value. However, the estimates of their average momentum are quite different, reflecting the difference of their quark constitution. Indeed, we find for $\pi$ and p

$$\frac{< P >_\pi}{< P >_p} = 0.686 \pm 0.024,$$

consistent with 2/3, which is the ratio of quark contents of $\pi$ and p. On the other hand, from the pairs of $\pi$ and K, we get

$$< P >_\pi - < P >_K = \frac{1}{2}(0.897 \pm 0.144) = 0.447 \pm 0.072 \text{ GeV},$$

comparable to the mass difference between the valence quarks s and u (or d).

Consider next the case of a resonance, e.g. $a \rightarrow b + c$. As the momentum distribution of the particle $a$ is given by the convolution of those of the decay particles b and c, we get the following relationship

$$\frac{1}{L_a} = \frac{1}{L_b} + \frac{1}{L_c}. \qquad \text{(A-1)}$$

Therefore, for $\rho^0 \rightarrow \pi^+ + \pi^-$, we expect $L_\varrho = L_\pi/2$, in agreement with the experimental values listed in the Table.

Likewise, for K*(892) $\rightarrow$ K + $\pi$, we find by the above relationship (A-1): $L_{K^*} = 0.099 \pm 0.018$ which agrees well with the experimental value $0.085 \pm 0.015$ within about 1/4 standard deviation.

Turn next to the $\gamma$'s, which are from the decays of $\pi^0 \rightarrow \gamma + \gamma$. Experimentally, however, both $\gamma$'s are recorded as independent particles, no account being taken of their origin from $\pi^0$ decays. Consequently, their spectrum resembles that of $\pi$, and, instead of $L_\gamma = L_\pi/2$ we find rather $L_\gamma \simeq L_\pi$ and $< P >_\gamma > \frac{1}{2} < P >_\pi$, as should be, probably due to the solid angle bias in the forward direction.

We therefore have the feeling that actually $L_\gamma = L_\pi/2$, i.e., $0.109 \pm 0.008$. This agrees with $L_\gamma = 2L_\eta = 0.102 \pm 0.042$, as the $\eta$'s are identified according to their decays: $\eta \rightarrow \gamma + \gamma$.

Finally, for electrons, as they arise from the pair production of $\gamma \rightarrow e^+ + e^-$, we expect $L_e = L_\gamma/2$ as has been found experimentally.

We now investigate the energy dependence of the average momentum $< P >$ for $\pi$, K and p. We have analyzed their momentum distributions at $E_{cm} = 10$, 29 and 91.2 GeV of the ARGUS Collaboration [17], the TPC and MARK II Collaborations [15,18] and the ALEPH [19] , DELPHI [20], L3 [21] and OPAL [22] Collaborations, respectively. The values of $< P >$ thus obtained are shown in Fig. 11, the plots of momentum distributions being omitted for simplicity.

As the average momentum is related to the multiplicity, which depends on the mass of the particle under consideration. Therefore its energy dependence follows a power law according to the statistical model of Fermi [12] and Landau [13]. Furthermore, assuming a Poisson distribution for the mass dependance, we may tentatively write

$$< P(m, E_{cm}) >= K(E_{cm})^\alpha \frac{m}{\mu} e^{-m/\mu}. \qquad \text{(A-2)}$$

where $\alpha$ and $\mu$ are two parameters and K a constant.

If we fit these three sets of data with (A-2) as shown in Fig. 11, we find the values of $1/\mu$ (in $(GeV)^{-1}$) increasing very slowly with energy as shown by the triangles in Fig. 12; the curve being a power law fit with

$$\frac{1}{\mu} = (0.991 \pm 0.013)(E_{cm})^{(0.150 \pm 0.003)}.$$

As the mean value of the estimates of $\mu$ as shown in Fig. 12, is $0.533 \pm 0.0526$ GeV, which turns out to be the same as that of the mass of the particles $\pi$, K and p, and as the parameter $\mu$ is not critical for the fit with (A-2), we therefore set

$$\mu = \frac{(m_\pi + m_K + m_p)}{3} = 0.525 \text{ GeV}$$

and redo the fits to estimate the parameter $\alpha$ and the factor $K(E_{cm})^\alpha$ of Eq.(A-2), the values thus obtained are presented by circles in Fig. 10. The curve represents the

fit using Eq. (A-2) with

$$\alpha = 0.716 \pm 0.050, \quad \mathrm{K} = 0.511 \pm 0.026. \tag{A-3}$$

We now try an overall fit with Eq.(A-2) using the parameters thus determined as shown by the solid curves in Fig. 11. A comparison with the data indicates that the fit is very satisfactory.

It is interesting to note that $\alpha \simeq 3/4$ so that the energy dependence of the average momentum behaves like the entropy as is expected from the viewpoint of the statistical model of particle production . On the other hand, at a given energy of production, the ratio of $< \mathrm{P} >$ for protons and pions leads to

$$\frac{< \mathrm{P} >_p}{< \mathrm{P} >_\pi} = \frac{m_p}{m_\pi} e^{-(m_p - m_\pi)/\mu} = 1.499 \simeq \frac{3}{2}.$$

equal to the ratio of quark contents of the proton and the pion, as mentioned before.

These properties of fundamental importance as revealed by the average momentum computed according to lognormal distribution justify, a posteriori, the relationship (A-2) for the mass and the energy dependence of the average momentum and the description of the momentum spectrum with the lognormal distribution (2) in terms of the invariant phase-space of the particle under consideration.

As regards the parameter $\zeta^*$, it represents the shift of the maximum of the momentum distribution in terms of Log(P). It has the property of scaling for a canonical transformation of (2) by substituting:

$$\mathrm{P} \rightarrow \alpha \cdot \mathrm{P}, \tag{A-4}$$

with

$$\alpha = \mathrm{antiLog}(\zeta^*),$$

so that the lognormal distribution Eq.(2) we have used to analyze the momentum spectra may be rewritten as follows

$$\frac{\mathrm{dn}}{\mathrm{dP}} = \mathrm{N} e^{-(Log[\alpha.P])^2/2L}. \tag{A-5}$$

In this form,the moments of P are given by integrating over $\zeta = \mathrm{Log(P)}$

$$M_n = 2.303\mathrm{N} \int 10^{(\alpha+n)\zeta} \frac{\mathrm{dn}}{\mathrm{dP}} \, d\zeta.$$

Finally, we note that for the kinematic variable of the lognormal distribution, if instead of the momentum, use is made of the kinetic energy as customarily adopted in the cosmic ray experiments, namely, Log P $\rightarrow$ Log(K + m), the fits become less good for particles heavier than kaons.

References and Footnotes


[1] E. Fermi, Phys. Rev. 75, 1169 (1949).

[2] E. Fermi, Astrophys. Journ. 119, 1 (1954).

[3] AMS Collaboration, J. Alcarez, et al., Phys. Lett. B 472, 215 (2000) and 490, 27 (2000).

[4] AMS Collaboration, J. Alcarez, et al., Phys. Lett. B 494, 193.

[5] AMS Collaboration, J. Alcarez, et al., Phys. Lett. B 484, 10 (2000).

[6] The spectrum index for electrons est estimated to be $\gamma_{e^-} = 3.176 \pm 0.088$ for $2.8 < P < 28$ GeV/c, so that the spectrum is much steeper than that of protons.

[7] T. T. Chou, Chen Ning Yang and Ed. Yen, Phys. Rev. Lett., 54, 510 (1985).

[8] CAPRICE Collaboration, M. Boezio, et al., Phys. Rev. D 62, 032007 (2000) and Astrophys. Journ. 532, 653 (2000).

[9] MASS Collaboration R. Bellotti, et al., Phys. Rev. D 60, 052002 (1999).

[10] BESS Collaboration, S. Orito, et al., Phys. Rev. Lett. 84, 1078 (2000).

[11] T. F. Hoang - Particle-antiparticle production of $e^+e^-$ and $\bar{p}p$ in Cosmic Rays, LBNL Report 52117.

[12] E. Fermi, Prog. Theor. Phys., 5, 570 (1950) and Phys. Rev. 81, 683 (1951).

[13] L. D. Landau, Akad. Nauk SSSR, ser., fiz., 17, 51 (1953).

[14] T. F. Hoang, (a) Zeit. Phys. C 63, 269 (1994) and (b) Phys. Rev. D 38, 2729 (1988).

[15] TPC Collaboration, H. Aihara, et al., Phys. Rev. Lett. 52, 577 (1984); Zeit. Phys. C 27, 39 (1985) and 187 (1985); and Phys. Lett. B 184, 299 (1987).

[16] HRS Collaboration, S. Abachi, et al., Phys. Rev. D. 40, 706 (1989) and Phys. Lett. B 199 (1987); and M. Derrick, et al., Phys. Rev. Lett. 54, 2588 (1985).

[17] ARGUS Collaboration, H. Abrecht, et al., Zeit. Phys. C, 444, 547 (1989) and Phys. Rep. 276, 223 (1996).

[18] MARK II Collaboration, A. Petersen, et al., Phys. Rev. D 37, 1 (1988) and H. Schellman, ibid., 31, 3013 (1985).

[19] ALEPH Collaboration, D. Buskulic, et al., Zeit. Phys. C 66, 355 (1995) and ibid., 64, 361 (1994).

[20] DELPHI Collaboration, P. Arino, et al., Phys. Lett. B 240, 171 (1990).

[21] L3 Collaboration, B. Adeva, et al., Phys. Lett. B 259, 199 (1991).

[22] OPAL Collaboration, R. Akers, et al., Zeit. Phys. C 63, 181 (1994).

Figure Captions

[1] Momentum spectrum of cosmic ray protons at 350 - 390 km altitude, AMS Collaboration [3-5]. The curve represents a least-squares fit with the lognormal distribution (2). The average momentum of protons is $2.316 \pm 0.022$ GeV/c.

[2] Plots of the average momentum vs. the cut-off on the momentum range for cosmic ray protons and $^4$He of the AMS Collaboration [3-5] the curves represent an exponential probability law, Eq. (4), leading asymptotically to the exact value of $< P > = 2.113 \pm 0.021$ GeV/c and $4.473 \pm 0.008$ GeV/c for protons and $^4$He, respectively.

[3] Momentum spectrum of cosmic ray $^4$He of the AMS Collaboration [4]. The curve represents a least-squares fit with the lognormal distribution (2). The average momentum of $^4$He measured by the magnetic spectrometer is estimated to be $4.558 \pm 0.0221$ GeV/c.

[4] Momentum spectrum of cosmic ray electrons and positrons of the AMS Collaboration [5]. The curves represent least-squares fits with the lognormal distribution (2). The average momentum of electrons is $2.153 \pm 0.118$ GeV/c and roughly $> 1.313 \pm 0.018$ GeV/c for positrons.

[5] Plots of the average momentum vs. the cut-off on the momentum range for cosmic ray electrons and positrons of the AMS Collaboration [5] the curves in dotted lines represent an exponential probability law, Eq. (4). The estimates of $< P >$ according to the plateau are $2.013 \pm 0.227$ GeV/c for electrons and $1.787 \pm 0.014$ GeV/c for positrons. The solid curve is another fit to electrons with $P < 3$ GeV/c (in filled circles) as in the case of positrons, leading to $1.781 \pm 0.014$ GeV/c the same as for positrons.

[6] Momentum spectrum of cosmic ray electrons and muons of the CAPRICE Collaboration [8]. The curves are fits with the lognormal distribution Eq. (2). The average momentum is $2.307 \pm 0.004$ GeV/c for the electrons and $2.163 \pm 0.205$ GeV/c for the muons.

[7] Log plot of momentum distributions of negative muons at various altitudes between 25 and 255 g/cm$^3$ of the MASS Collaboration [9]. The curves are lognormal fits with Eq. (2). The parameters and the estimates of the average momentum are listed in Table I.

[8] Plot of the negative muon flux (in particles/$(cm^2 ssr)$) vs. altitude x (in g/cm$^3$) of the MASS Collaboration [9]. The solid curve represents a linear fit $n_\mu = x/(7205 \pm 167)$ , see text.

[9] Momentum distributions of $\pi^+\pi^-$, $\gamma$, $e$, $K^+K^-$ from $e^+e^-$ collisions at $E_{cm}$ = 29 GeV, TPC Collaboration [14]. The curves are least-squares fits with the lognormal distribution Eq. (2). The parameters and the estimates of $< P >$ are listed in Table II of Appendix.

[10] Momentum distributions of $\rho^0$, $\eta$, and $K^{+*}K^{-*}$ from $e^+e^-$ collisions at $E_{cm}$ = 29 GeV, HRS Collaboration [15]. The curves are least-squares fits with the lognormal distribution Eq. (2). For the parameters and the average momentum, see the text in Appendix.

[11] Plots of the average momentum (in GeV/c) of $\pi^{\pm}$, $K^{\pm}$, p against the secondary mass m (in GeV) for $e^+e^-$ collisions at $\sqrt{s}$ = 10, 29 and 91.2 GeV' of ARGUS, PEP and LEP experiments [17-22]. The curves represent an overall fit according to (18) with 2 free-parameters, $\mu = 0.533$ GeV and $\alpha = 0.716$ for the mass and the energy dependence of the computed average momentum, see Appendix.

[12] Plots of the parameter $1/\mu$ (in triangles) and the estimate $K(E_{cm})^{\alpha}$ (in circles) for $< P >$ as expressed by (18), as a function of the energy $E_{cm}$ (in GeV) of $e^+e_-$ collisions for $\pi$, K and p. The curves are power-law fits, see text (Appendix).

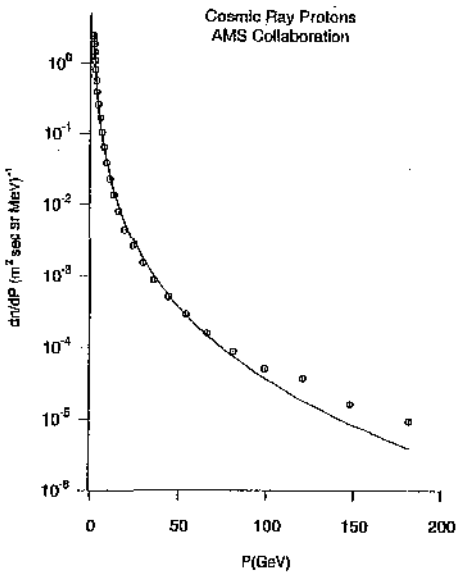
Cosmic Ray Protons
AMS Collaboration
dn/dP (m² sec sr MeV)⁻¹
P(GeV)

Fig. 1

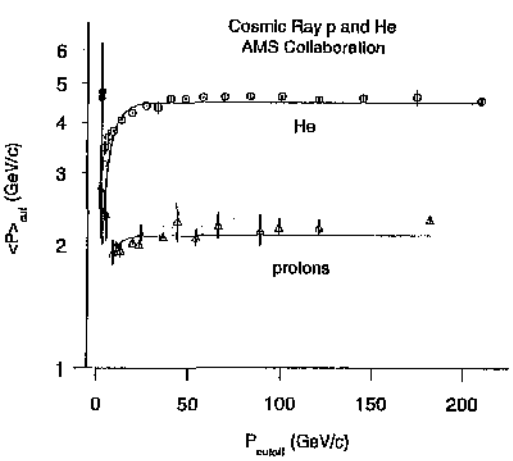
Cosmic Ray p and He
AMS Collaboration
He
protons
<P>cut (GeV/c)
Pcutoff (GeV/c)

Fig. 2

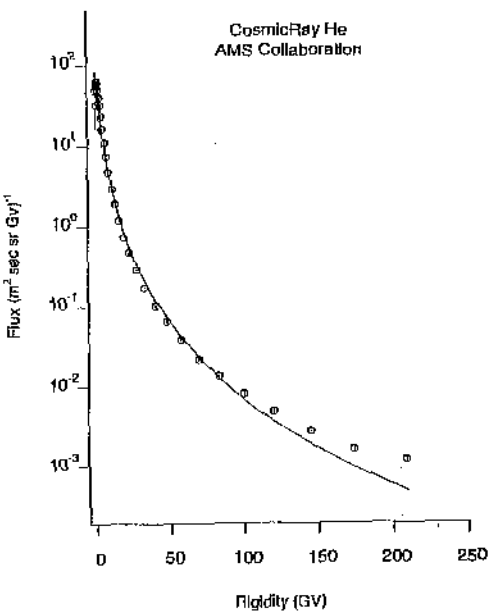
CosmicRay He
AMS Collaboration
Flux (m² sec sr Gv)⁻¹
Rigidity (GV)

Fig. 3

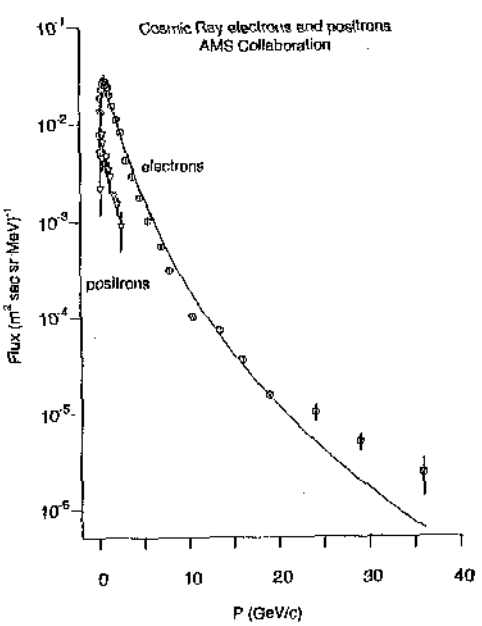
Cosmic Ray electrons and positrons
AMS Collaboration
electrons
positrons
Flux (m² sec sr MeV)⁻¹
P (GeV/c)

Fig. 4

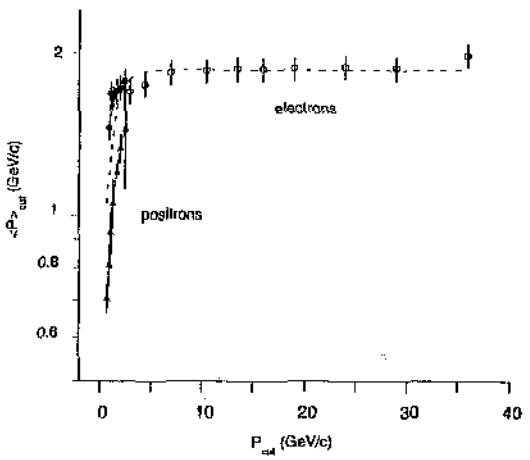
2
1
0.8
0.6
electrons
positrons
0
10
20
30
40
$P_{out}$ (GeV/c)

Fig. 5

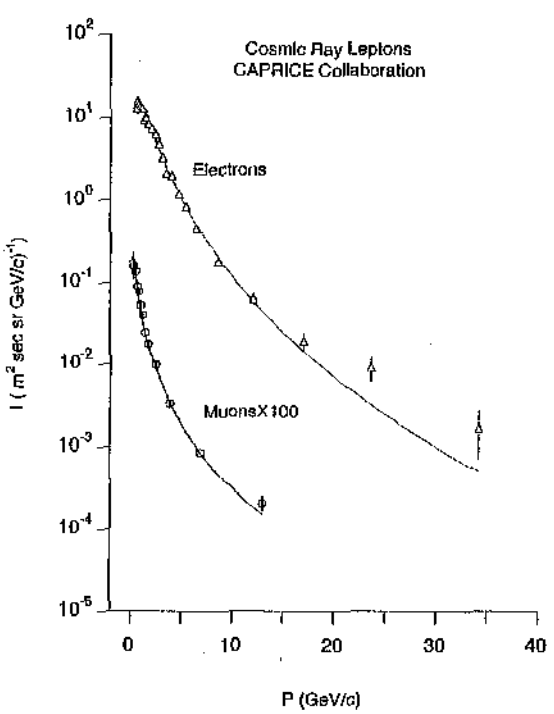
Cosmic Ray Leptons
CAPRICE Collaboration
Electrons
MuonsX100
I ( $m^2$ sec sr GeV/c)$^{-1}$)
P (GeV/c)
0
10
20
30
40

Fig. 6

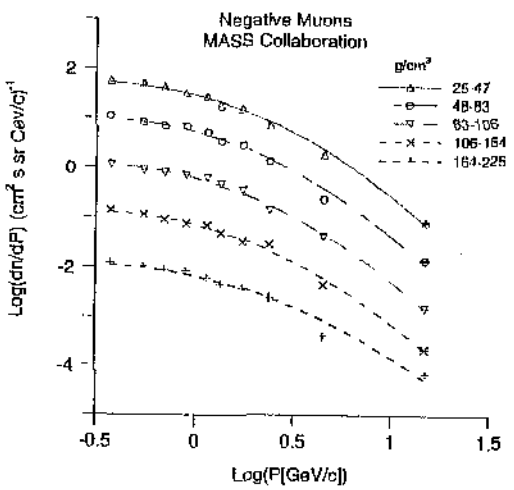
Negative Muons
MASS Collaboration
g/cm²
25-47
48-83
83-106
106-164
164-225
Log(dn/dP) (cm² s sr Gev/c)⁻¹
Log(P[GeV/c])
2
0
-2
-4
-0.5
0
0.5
1
1.5

Fig. 7

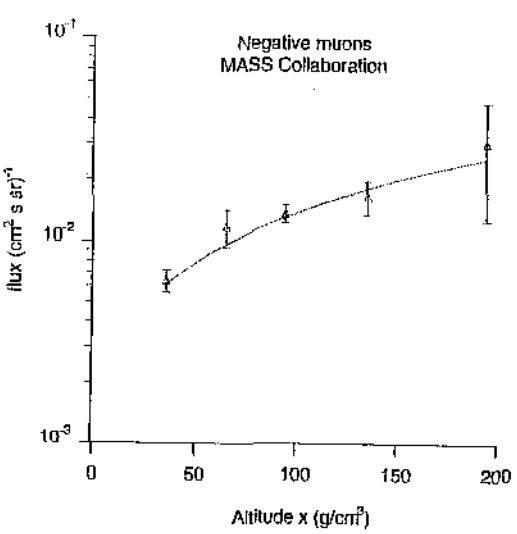
Negative muons
MASS Collaboration
flux (cm² s sr)⁻¹
Altitude x (g/cm²)
10⁻¹
10⁻²
10⁻³
0
50
100
150
200

Fig. 8

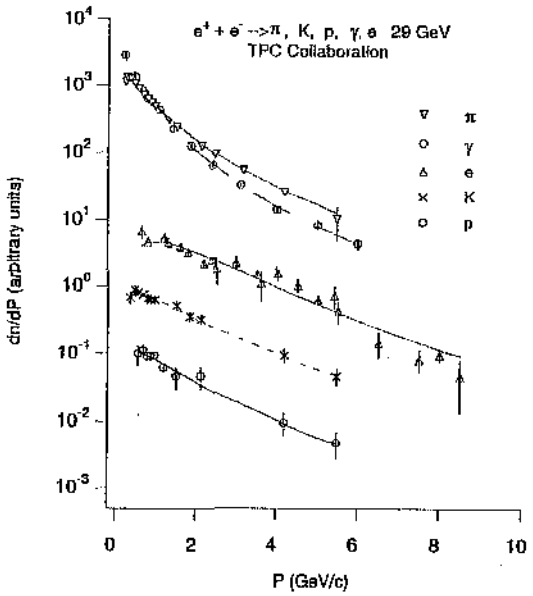
e+ + e- -->π, K, p, γ, e 29 GeV
TPC Collaboration
π
γ
e
K
p
dn/dP (arbitrary units)
P (GeV/c)

Fig. 9

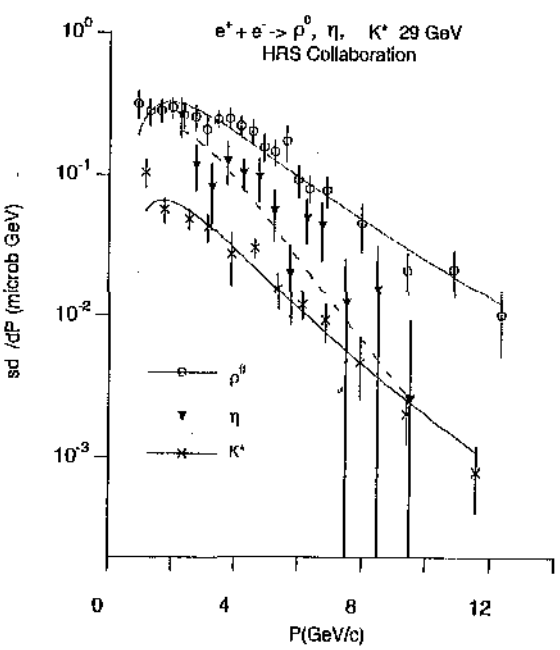
e+ + e- -> ρ0, η, K* 29 GeV
HRS Collaboration
ρ0
η
K*
sd /dP (microb GeV)
P(GeV/c)

Fig. 10

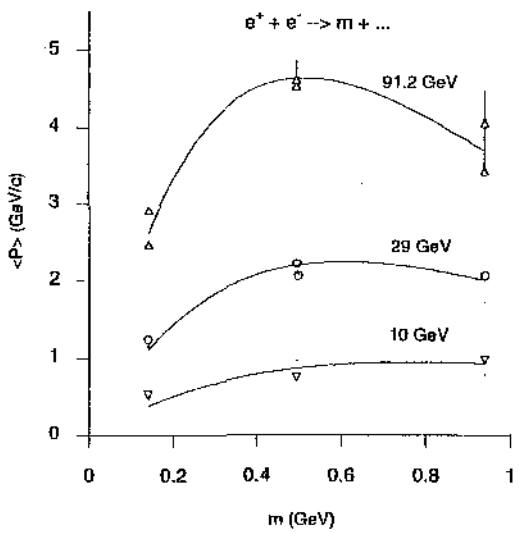
e+ + e- --> m + ...
91.2 GeV
29 GeV
10 GeV
<P> (GeV/c)
m (GeV)
0
1
2
3
4
5
0.2
0.4
0.6
0.8

Fig. 11

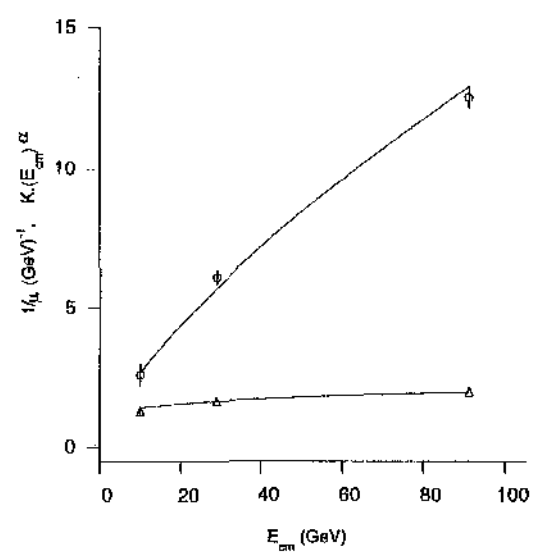
1/μ (GeV)-1 , K.(Ecm) α
Ecm (GeV)
0
5
10
15
20
40
60
80
100

Fig. 12